

EFFECT OF MgO ADDITION ON THE SUPER CONDUCTING PROPERTIES OF (Bi-Pb)-2223/Ag TAPES AND ECONOMIC ASPECTS RELATED TO SUPERCONDUCTORS

¹Praveen K.H, ²Soumya Viswambharan

¹Assistant Professor of Physics, ²Assistant Professor of Economics

¹²Sree Narayana College Punalur, Kerala, 691305, India

Abstract: Among the several families of high T_c ceramic superconductors, (Bi,Pb)-Sr-Ca- Cu-O system has attracted the attention for the fabrication of super conducting wires and tapes. In this system, the identified superconducting phases are Bi-2201 ($T_c = 10K$), Bi- 2212 ($T_c = 85K$) and Bi-2223 ($T_c = 110 K$). Of these, the Bi-2223 phase offers a large temperature window for 77K operation. Considerable effort has been made by various groups during the last few years to fabricate super conducting tapes with Bi-2223 phase by several techniques. The powder-in-tube (PIT) technique has assumed greater significance because of the superior performance of the processed tapes, particularly with respect to the transport properties and the ease of the fabrication of long flexible tapes. Such tapes are being produced with consistently high critical current values of around 30,000 A/cm² at 77K and zero field for short length. Producing superconducting materials, particularly high-temperature superconductors (HTS), is expensive.

Index Terms – High T_c ceramic superconductors, BPSCCO, (Bi,Pb)- 2223/Ag super conducting tapes, ultrafine MgO doping, fluxpinning centres, intermediate annealings, powder-in-tube (PIT) technique, sol-gel synthesis, Economic aspects etc.

INTRODUCTION

Ag-sheathed Bi – 2223 tapes can give the largest critical currents of all high T_c superconductors that can be of practical use. Unfortunately, the J_c of these materials are sensitive to magnetic fields due to weak links between the grains [in the low field regime (≤ 1 mT) and at higher temperatures], due to insufficient flux pinning (in the high field regime and at lower temperatures). The weak-links can be minimised by careful optimization of the processing steps. Flux pinning strength can be improved by the addition of fine second phase particles [1], ion-neutron or γ -ray induced damage zones [2] or by careful optimization of thermo-mechanical treatments [3]. Because the coherence length in high- T_c superconductors is so small, the dimension of the pinningcentres (defects, dislocations, second phase particles, etc.) also should be of the same order.

The present experiment aims at the effect of fine MgO addition in different percentages on the superconducting properties and phase evolution of (Bi,Pb)- 2223/Ag tapes. It is reported that ultrafine MgO particles can act as flux pinners in BPSCCO system [4]. J. Schwartz et al. and Linghua et al. have investigated the effect of ultrafine MgO doping on various superconducting properties of Bi-2223/Ag tapes (PIT), and a brief summary is given below. [1,4]

X-ray diffraction analysis showed that Bi-2223 phase formation is slowed down because of MgO addition, which to a certain extent is beneficial to the grain connectivity and grain alignment in fully processed samples. The transport critical current in 1 wt% MgO doped samples sintered at 835°C or 839°C is improved significantly compared to the undoped samples. This observation suggests that, the ultrafine MgO particles might act as fluxpinning centres and thus reduce the flux creep effectively. The advantage of MgO is that it is non-reacting with BPSCCO and can survive the heat treatment without degrading T_c , J_c , etc.

The powder was prepared by sol-gel method following an acrylate route. High purity oxides/carbonates (>99.99%) viz Bi₂O₃, PbO, SrCO₃, CaCO₃ and CuO are weighed to prepare 40g of precursor powder according to the stoichiometry of Bi_{1.8} Pb_{0.4} Sr₂ Ca_{2.2} Cu_{3.1} O_x.

Preparation of MgO doped (Bi-Pb)-2223/Ag tapes

To study the effect of MgO addition, it is added to the precursor powder in different weight percentages such as 0.5%, 1%, 2% & 4% and ground homogeneously in acetone medium. Ag - clad tapes were fabricated by powder-in-tube (PIT) technique. Ag was used as sheath material because of its low reactivity with the superconductor, good electrical and mechanical properties and its ability to diffuse oxygen. The pure precursor powder and the four MgO added samples were packed into high purity (99.99%) seamless Ag- tubes (OD = 10mm, ID = 7.0mm, length = 3cm) with a packing density of around 3.2 g/cc. The ends of the tubes were closed with suitable Ag-plugs and crimp-sealed after an annealing (500°C) to remove any entrapped moisture, the tubes were rolled through a series of grooves to a diameter of 1.4 to 1.5 mm with intermediate annealings. The wire was then flat-rolled into tapes of thickness around 280 μ m with intermittent rolling-cum-annealings. The heat treatment of all the tapes was done in the temperature range 830- 840°C for various durations ranging from 0-200h. The heat treatments of all the samples were carried out in a muffle furnace in which, the temperature

was controlled to an accuracy and stability of $\pm 1^{\circ}\text{C}$, employing programmable temperature controllers. The final thickness of the tapes thus prepared was around $150\text{ }\mu\text{ m}$.

XRD Analysis

The phase evolution of the precursor powder and the tape core (after 50h, 100h & 200h of heat treatments) was studied by an automated x-ray diffractometer (Philips PW 1710) using Cu K- α radiation. The basic principle of x-ray powder diffraction is the Bragg's law, which states that, $2d \sin \theta = n \lambda$, where n is the order of diffraction, d is the interplanar spacing, λ is the x-ray wave length used and θ is the angle of diffraction.

The powder filled sample holder is kept at the centre of the vertical goniometer cell of the diffractometer. The diffractometer is designed to disperse x-rays of a single wave length by diffracting them from planes of different spacing. The x-ray generator is operated at 40 kV and 20 mA

The phase evolution study was done by comparing the peak intensities of the selected peaks of the representative phases such as Bi-2223 ($2\theta = 24.05$), Bi-2212 ($2\theta = 23.1$), Bi-2201 ($2\theta = 29.8$), Ca_2PbO_4 ($2\theta = 17.81$), CuO ($2\theta = 38.99$), Ca_2CuO_3 ($2\theta = 36.37$). The volume fraction of the individual phase was taken as the ratio of intensity of the representative peak of the particular phase to the total intensity of the representative peaks of all the phases present.

Critical current density (J_c) measurement

The transport critical currents of the tapes at 77K are measured by the ‘four-probe method’ in liquid Nitrogen using a $1 \mu\text{V cm}^{-1}$ criterion (fig 3.1). A constant DC source having a capacity of 30A supplied the desired current and a nano voltmeter (Keithely 181) was used to measure voltage. The instruments are interfaced through a PC and data collection was performed using appropriate software. The voltage leads were soldered on the tapes 1cm apart and the voltage drops between the leads were measured using the nanovoltmeter. As universally accepted, J_c is defined as the current density which develops a fixed value of electric field (usually $1 \mu\text{V cm}^{-1}$) on the surface of the superconductor.

Jc- B Measurement

Dependence of critical current density on applied magnetic field is a very important characteristic. At low field strengths, the measurement may yield information on weak-links. At intermediate strengths, information on inter-granular flux pinning and in strong fields, the information on flux lattice melting can be obtained. The experimental set up is same as explained for the J_c measurement. The field was applied to the ab-plane of the tape. Here the field was produced by a pair of home-made Cu wound electromagnets, with provision for varying the field.

DISCUSSION

Fig.I shows the XRD pattern of the precursor powder. The different phases identified in the pattern are (a) Bi-2201, (b) Bi-2212, (c) Ca_2PbO_4 , (d) CuO and (e) Ca_2CuO_3 . From the pattern, it is clear that Bi-2212 is the prominent phase.

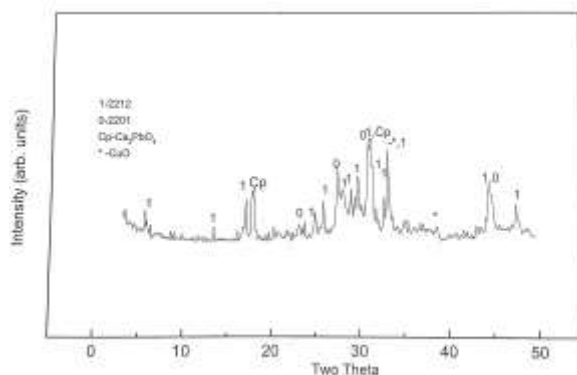


Fig. 1: X-Ray Diffraction patterns of the precursor powder

Fig.II shows the SEM picture of the precursor powder. It can be seen that the average particle size is around 1-2 μm .



FIG II

Table3. I gives the volume fractions of different phases of the tapes heat treated for different durations viz. 50h, 100h, and 200h respectively. The phases identified are Bi₂223, Bi-2212, Bi2201, Ca₂PbO₄, CuO and Ca₂CuO₃. Here, for each sample, the fraction of Bi-2223 phase increase as it passes different stages of heat treatments (50 h, 100 h and 200 h). It can be seen that the volume fraction of Bi-2223 is the greatest for the pure sample and slightly decreases as the MgO percentage is increased. The fraction is the least for 4wt% MgO added sample. This can be explained as follows; as the MgO percentage increases, it may deteriorate the growth of Bi-2223, as MgO particles may agglomerate in the core. It can also be seen that, the non-super conducting impurity phases such as Ca₂PbO₄, Ca₂CuO₃ and CaO present in all samples in notable amounts.

| Table 3.1 | 1. Pure sample | | | 2. Pure sample + 0.5wt% MgO | | | 3. Pure sample + 1 wt% MgO | | | 4. Pure sample + 2 wt% MgO | | | 5. Pure sample + 4 wt% MgO | | |
|----------------------------------|----------------|-------|-------|-----------------------------|-------|-------|----------------------------|-------|-------|----------------------------|-------|-------|----------------------------|-------|-------|
| Phases | 50 h | 100 h | 200 h | 50 h | 100 h | 200 h | 50 h | 100 h | 200 h | 50 h | 100 h | 200 h | 50 h | 100 h | 200 h |
| Bi-2223 | 20.01 | 56.18 | 86.30 | 20.8 | 56.19 | 84.20 | 19.22 | 53.40 | 83.70 | 17.30 | 50.14 | 78.00 | 16.50 | 50.00 | 76.20 |
| Bi-2212 | 36.72 | 11.36 | 2.90 | 36.00 | 11.31 | 2.80 | 36.70 | 10.90 | 2.10 | 34.9 | 9.20 | 2.21 | 34.70 | 11.90 | 2.01 |
| Bi-2201 | 17.69 | 12.87 | 1.60 | 17.80 | 12.69 | 1.67 | 17.10 | 14.20 | 1.20 | 19.65 | 16.47 | 4.90 | 21.00 | 17.62 | 2.50 |
| Ca ₂ PbO ₄ | 13.17 | 10.94 | 5.00 | 13.00 | 10.86 | 6.10 | 12.90 | 11.70 | 7.60 | 12.76 | 11.60 | 6.58 | 13.50 | 10.80 | 7.98 |
| Ca ₂ CuO ₃ | 6.12 | 3.80 | 2.29 | 5.65 | 3.79 | 2.46 | 6.69 | 4.29 | 2.30 | 6.53 | 5.58 | 3.51 | 7.00 | 5.47 | 5.10 |
| CuO | 6.50 | 4.82 | 1.91 | 6.48 | 4.79 | 2.77 | 7.39 | 5.51 | 3.10 | 8.86 | 7.01 | 4.90 | 7.30 | 4.21 | 7.21 |

Table 3.1. The volume fraction of samples

Fig. III shows the XRD patterns of the tape samples after 50h heat treatment. Here, the pure sample shows the highest peak for Bi-2223 phase and its height decreases as the percentage of MgO is increased. The patterns show no significant difference in the case of other phases. In this pattern, the peak of the Bi-2212 is the prominent peak.

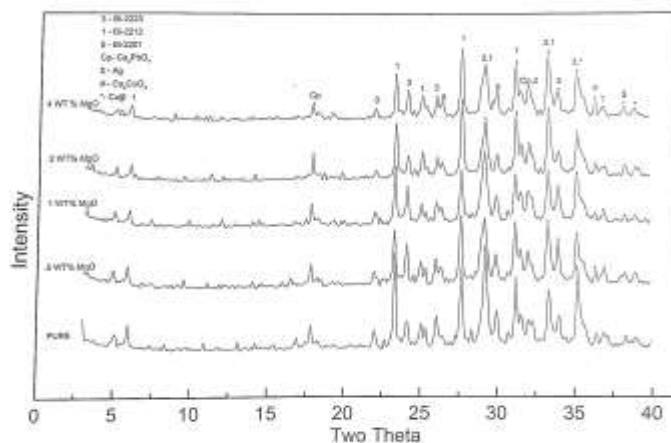


Fig. III. X-Ray diffraction patterns of the MgO added tapes after 50H

Fig. IV shows the XRD s of the tape samples after 100h heat treatment. Here also the pure sample gives the largest peak for Bi-2223 phase. Bi-2212 peak is much lowered in this pattern.

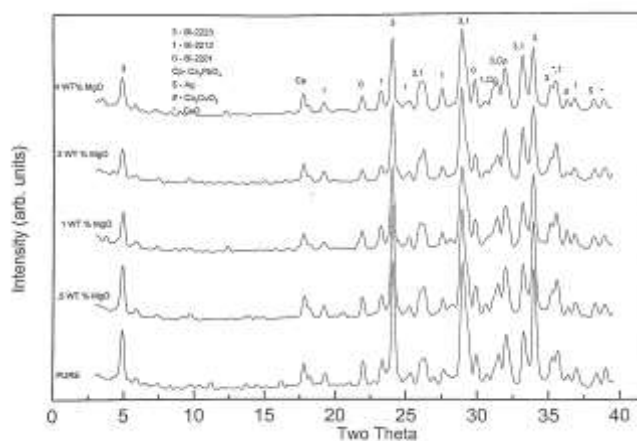


Fig. IV. X-Ray Diffraction patterns of the MgO added tapes after 100h

Fig. V shows the XRD pattern of the tape samples after 200h heat treatment. Therealso, no significant difference between the samples. Bi-2223 phase have the most prominent peak and its intensity decreases from pure to the last sample.

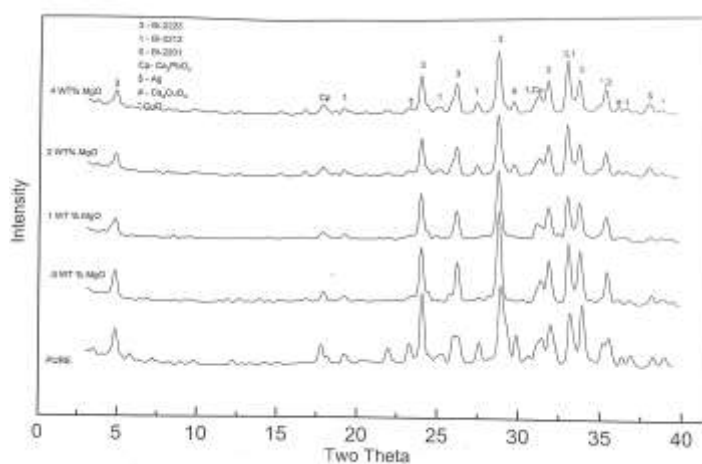


Fig.V. X-Ray Diffraction pattern of the MgO added tapes after 200h

Fig. VI shows the plots of J_c (kA/cm²) values of different samples for different intervals of heat treatment viz. 100h,150h and 200h. It reveals that the J_c value is the highest for the pure sample after complete heat treatment. For samples (Pure + 0.5) and (Pure + 1), the J_c values are comparable and it is lower for samples (Pure +2) and (Pure +4).

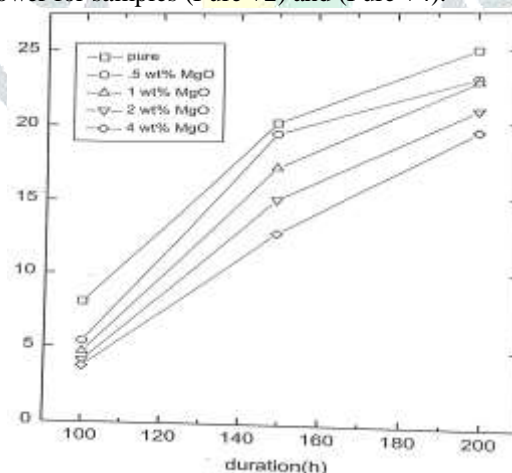


Fig. VII is the plot of normalized I_c [$I_c(B) / I_c(0)$] as a function of the applied field. The graph indicates slightly higher values of the normalized I_c for the pure sample. Inset of fig VII shows the variation of normalized I_c at low field region (0 to 100G). Within the present experimental limits, the flux pinning effect of MgO could not be observed as it require still higher fields and lower temperatures.

Economic aspects related to superconductors

1. Production Costs

Superconductors, while offering remarkable properties such as zero electrical resistance and the ability to carry current without loss, are not yet economically viable for widespread use. This is primarily due to several key challenges:

High temperature superconductors often require rare or expensive materials, such as Yttrium, Barium, Copper oxide etc. Superconductors typically require advanced manufacturing techniques, such as precise thin-film deposition or complex alloying processes. For instance, making thin-film, wires or tapes, superconductors involves high-energy methods, such as pulsed laser deposition or sputtering, which can be expensive and energy-intensive. Complexity of Fabrication: Producing superconducting wires, cables, or other devices requires precise control of the material's microstructure. Achieving the required purity, composition, and structural alignment can involve highly sophisticated equipment and processes, driving up costs.

2. Cooling and Operational Costs

Cryogenic Cooling: One of the most significant challenges in the economics of superconductors is the need for cooling to extremely low temperatures. Most superconductors require cooling with liquid helium or nitrogen, which adds substantial operating costs. Even high-temperature superconductors (which operate at "higher" temperatures, such as -135°C or -196°C) still require cooling with liquid nitrogen, which is expensive to produce and store.

Energy Costs: The energy required to cool superconductors can often exceed the energy savings gained from their zero-resistance properties. The cost of cryogenic systems, including refrigeration and insulation, can be very high. Although research is ongoing to find room-temperature superconductors, most current high-temperature superconductors are still far from being cost-effective for everyday use.

3. Infrastructure Costs

The large scale implementation of superconductors in power grids or transportation systems would require a massive investment in infrastructure. Replacing conventional electrical cables with superconducting cables or building large-scale superconducting magnets (used in projects like maglev trains or MRI machines) requires specialized infrastructure, which is capital-intensive. To fully integrate superconductors into power grids, substantial upgrades to energy distribution systems would be needed, including specialized cooling equipment, protection systems, and controls. These infrastructure changes can be prohibitively expensive.

Superconductors are challenging to scale for widespread commercial use. For example, current superconducting wires and cables are often limited by their length, size, and cooling requirements, making large-scale deployment difficult and expensive.

4. Limited Market Applications

Currently, superconductors are used in a limited number of high-value, specialized applications. Superconducting magnets are used in medical imaging (MRI), but the cost of producing superconducting magnets for these machines is high. However, because MRI technology is critical for healthcare, the added cost is justified. Superconductors are also used in particle accelerators like the Large Hadron Collider (LHC), where their high performance and efficiency are essential. But again, these applications are niche and require substantial investment.

The field of quantum computing also relies on superconductors. However, the development of quantum computers is still in its early stages, and the costs associated with these technologies remain high. Large-scale, practical quantum computers will require breakthroughs in superconducting materials to be economically viable. Some transportation systems, like maglev trains, use superconducting magnets to levitate and propel trains at high speeds. However, maglev systems are limited to certain regions due to the high infrastructure and operational costs.

5. Potential Future Benefits

Despite current limitations, superconductors have the potential to revolutionize industries in the future, especially if technological advancements can reduce costs. Superconducting materials can transmit electricity without any energy loss due to resistance. This could dramatically improve the efficiency of power grids, reducing waste and lowering energy costs in the long term. Superconducting magnetic energy storage (SMES) systems could offer highly efficient energy storage solutions. This would be crucial for balancing renewable energy sources (like solar and wind) and ensuring a stable energy supply. Maglev trains and superconducting motors could reduce energy consumption in transportation and potentially lower the cost of travel, especially in high-speed rail systems. Superconducting circuits could lead to faster and more efficient computers, including quantum computers that may revolutionize industries like cryptography, materials science, and artificial intelligence.

6. Market Barriers

Competition from Conventional Technologies: Traditional conductors, such as copper and aluminum, are much cheaper and easier to produce. While superconductors offer efficiency advantages, the high costs of implementation and infrastructure make them less competitive for most applications, especially when resistance-based losses are tolerable.

Superconducting technologies are still evolving, and many applications are not yet commercially viable on a large scale. This limits the economic impact and widespread adoption of superconductors. Advances in cryogenics may provide more affordable and efficient cooling systems, reducing the operational costs associated with superconducting technologies. The economic benefit is often outweighed by the high cost of their production and maintenance. In many cases, traditional conductors like copper or aluminum, while

less efficient, are more practical and cost-effective for many applications. The energy loss due to resistance in these materials is manageable, and their manufacturing processes are well-established and inexpensive.

CONCLUSION

The effect of MgO addition in Ag/(Bi,Pb)-2223 superconducting tapes on phase evolution and superconducting properties was studied by fabricating the tapes with different percentages of nanosize MgO particles by powder-in-tube (PIT) technique. Characterization of the tapes by XRD analysis, and J_c measurement at 77K and self-field showed that,

- (1) No significant change either in the volume fraction of Bi-2223 or in the transport critical current density was observed among the MgO added samples (up to 4 weightpercentage), compared to the pure sample.
- (2) As the weight percentage of MgO increases, the superconducting properties of the samples slowly decrease. It is likely that, the nanosize MgO particles agglomerate into larger particles which subsequently segregate into (Bi, Pb)-2223 grain boundaries. This can hinder the (Bi, Pb) -2223 phase formation as well as the transport I_c .
- (3) Since there is a slight decrease in the volume fractions of Bi-2223, for MgO added samples there is a corresponding degradation of J_c , as the percentage of MgO increases. (Probably, due to the agglomeration and subsequent segregation of MgO particles in the grain boundaries which inhibit the transport current density).
- (4) The J_c -B characteristics of all the samples were found to be more or less same, with in the range of the magnetic field used in the present studies. Possibly, at higher fields (≥ 10 T) and lower temperatures, the flux pinning effect of MgO could be demonstrated.
- (5) The economics of superconductors are shaped by several factors, including production costs, material availability, operational requirements, and the potential for large-scale implementation. While superconductors offer significant advantages in terms of performance, their high costs have thus far limited their widespread adoption.

References

1. J. Schwartz, U.P. Trociewitz, W. Wei, P.V.P.S.S. Sastry B.T. Boutemy and P.R.Sahm IEEE transactions on magnetics (accepted 1998)
2. B.A. Albiss, M.K. Hasan, M.Aal-Akhras, I.A Al-Omari, A.Shariah, J.Shobaki, K.A. Azez, H. Ozakan, Physica C 331 (2000) 297 –301
3. J.Horvat, R. Bhasak, Y.C. Guo, H.K. Liu and S.X. Dou, Superconducting science and Technology 10 (1997) 409-415
4. Ling Hua, Jaimoo Yoo, Jue Woong Ko, Huidookim, Hyungsik chung, Guiwen Qiao. Physica C 291 (1997) 149-154
5. U. Syamaprasad, M.S. Sarma, A.R. Sheeja Nair, P. Guruswamy, P.S. Mukherjee, J. Koshy and A.D. Damodaran, R.R.L, Tvpms Bulletin of materials science, Vol.18, No.5, Sep1995, Pages 517-529.
6. R.P. Aloysius, A. Sobha, P. Guruswamy, K.G.K. Warriar, U. Syamaprasad, R.R.L, Tvpms, Physica C 328 (1999), Pages 221-229
7. Wangshui Wei, Yan gren Sun, Justin Schwartz, K. Goretta, U. Balachandran and A.Bhargava. IEEE transactions on applied superconductivity, Vol.7.No.2 June 1997.
8. L.S Lysam Ko, Y.V.Gomaniuk, I.P. Tya Gulski, I.N. Osiyuk, V.L.Lofovski and V.N.Varyukhiu. Physica C 281 (1997) Pages 303-309
9. M.Kichi, A.Yamasaki, T. Matsushita, J. Fujikami, K. Ohmatsu Physica C 315 (1999) Pages 241-246
10. J. Horvat, Y.C. Guo, S.X. Dou, Physica C 271 (1996) Paged 59-66.
11. Economic Feasibility of Superconducting Power Transmission by J.R. Williams and J.M. Moore, IEEE Transactions on Applied Superconductivity
12. The Economics of Superconducting Magnets for Fusion Energy by J. L. Cima and R. B. Garfield, Fusion Science and Technology